HIGH CURRENT BETATRON RESEARCH AT THE UNIVERSITY OF NEW MEXICO

S. Humphries, Jr. and L.K. Len
Institute for Accelerator and Plasma Beam Technology
University of New Mexico
Albuquerque, New Mexico 87131

1. Introduction

Betatrons are among the simplest of high energy accelerators. Their circuit is equivalent to a step-up transformer; the electron beam forms a multi-turn secondary winding. Circulation of the beam around the flux core allows generation of high energy electrons with relatively small core mass. As with any transformer, a betatron is energy inefficient at low beam current; the energy balance is dominated by core losses. This fact has prompted a continuing investigation of high current betatrons as efficient, compact sources of beta and gamma radiation [1].

A program has been supported at the University of New Mexico by the Office of Naval Research to study the physics of high current electron beams in circular accelerators and to develop practical technology for high power betatrons [2]. Fabrication and assembly of the main ring was completed in January of this year. In contrast to other recent high current betatron experiments [3,4] the UNM device utilizes a periodic focusing system to contain high current beams during the low energy phase of the acceleration cycle. The reversing cusp fields generated by alternating polarity solenoidal lenses cancel beam drift motions induced by machine errors. In consequence, we have found that the cusp geometry has has significantly better stability properties than a monodirectional toroidal field. In comparison to other minimum-B geometries such as the Stellatron [5], cusps have open field lines which facilitate beam injection and neutralization.

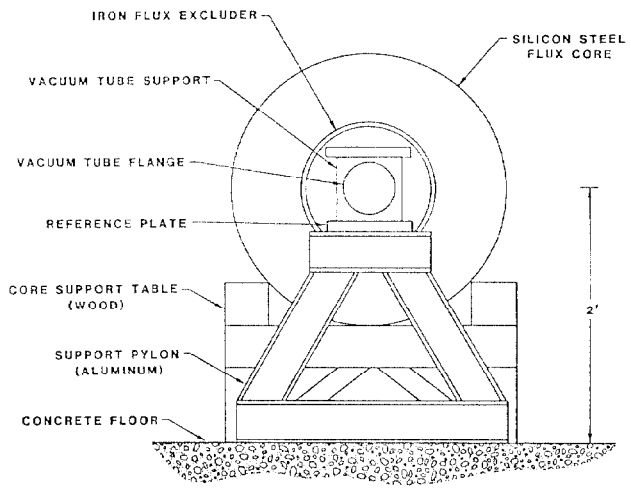

Fig. 1. Cross section of main ring, UNM Betatron.

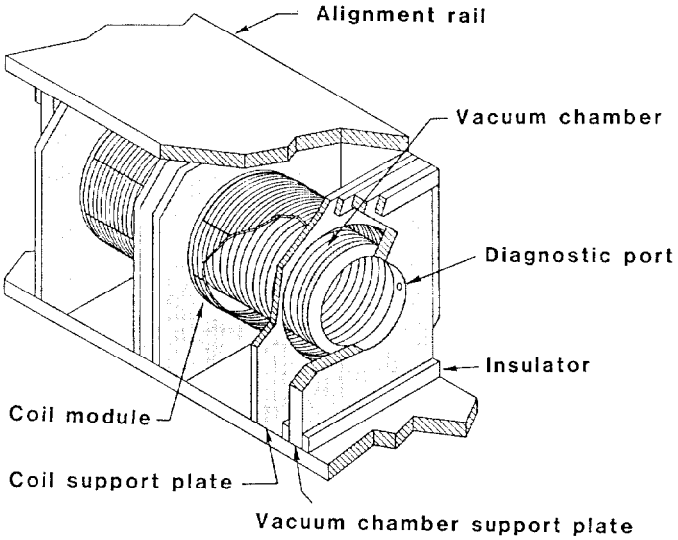

Fig. 2. Construction details of main ring, UNM Betatron.

A number of technical innovations have been incorporated in the UNM Betatron to achieve high energy efficiency and to optimize the versatility of the machine as a research device. Modular construction techniques have been used for all machine systems. For example, the device can be configured either as a racetrack with external injection or as a circular accelerator with an internal electron source. The technology of the main acceleration ring, high voltage injector, and beam inflector are reviewed in the following section. Experimental results on the performance of the injector, and high current transport in a linear periodic system are summarized in Section 3. Section 4 describes measurements of beam transport in a 180^{o} betatron sector. Presently, the machine is set up in a closed circular configuration. Transport of 50 keV electrons around the full circumference has been confirmed. Experiments are currently being performed on the acceleration of runaway electrons from a preionized, cusp contained plasma.

2. Features of the UNM Betatron

The main acceleration ring of the UNM betatron is illustrated in Fig. 1. Inductive isolation is provided by modular toroidal transformer cores. The ten cores are fabricated from 3000 turns of 4 mil silicon steel for fast pulse response. The volt-second product of the cores implies a maximum beam energy of 15 MeV for the 8 m circumference device. The accelerator output energy can be extended to 30 MeV with additional cores. The support system for the cores is mechanically independent of the precision alignment system for the main ring.

CH2387-9/87/0000-0914 $1.00 © IEEE

Fig. 2 is a detailed view of the main ring. The vacuum chamber consists of 18 stainless steel bellows assemblies with 13 mil wall thickness. The all-metal chamber construction avoids problems of beam space charge induced breakdowns. The vacuum chamber is interrupted by two re-entrant acceleration gaps. The bellows assemblies are supported by rigid plates with two diagnostic ports per plate.

Magnetic fields for beam bending and focusing are applied by 36 coil modules. Each module contains independent solenoidal and vertical field windings with low mutual inductance. The vertical field windings generate a sector field that can rapidly penetrate the thin vacuum chamber wall. The winding geometry was designed for highly uniform horizontal deflection over a 5 cm width. The properties of the fast isolation cores, thin vacuum chamber and sector-type vertical fields are compatible with acceleration cycles as short as 20 microseconds. The modular coils can be connected in various series-parallel combinations to achieve a wide range of risetimes for the focusing and acceleration fields. The coils are designed for applied voltage up to 10 kV.

The main ring components are mounted on 2 m diameter aluminum rails fabricated on a vertical mill. The vacuum chamber supports are isolated from the rails with insulating spacers to force beam return currents through the bellows. Vacuum pumping is performed by an 8" cryopump and an 8" ion pump. Pulsed power for the focusing fields, vertical fields and beam acceleration is supplied by two ignitron controlled 5 kJ capacitor banks. The acceleration bank is sufficient for beam loads to 2 kA. The acceleration cycle of the betatron and injector is computer controlled by a CAMAC system.

A variety of beam formation techniques, both in plasma and high vacuum environments, will be studied. The baseline technique involves trapping of a high energy beam (150 A, 300-600 keV) by pulsed, transverse electric fields. The beam inflector assembly, located in the 1 m racetrack section, is shown in Fig. 3. It consists of a magnetically shielded injection chamber and two 46 cm long electrodes that extend through three focusing cells of the downstream transport tube. The magnitude of the applied electrode voltage is 40 kV. The beam enters through a slot in the positively biased upper electrode. After the beam fills the betatron, the electrodes are rapidly shorted together by a distortion spark gap triggered by a delayed pickoff from the injector voltage. The beam is carried from the HV injector through a 1 meter long, 3.4 cm diameter transport tube with a 25 cell periodic focusing system.

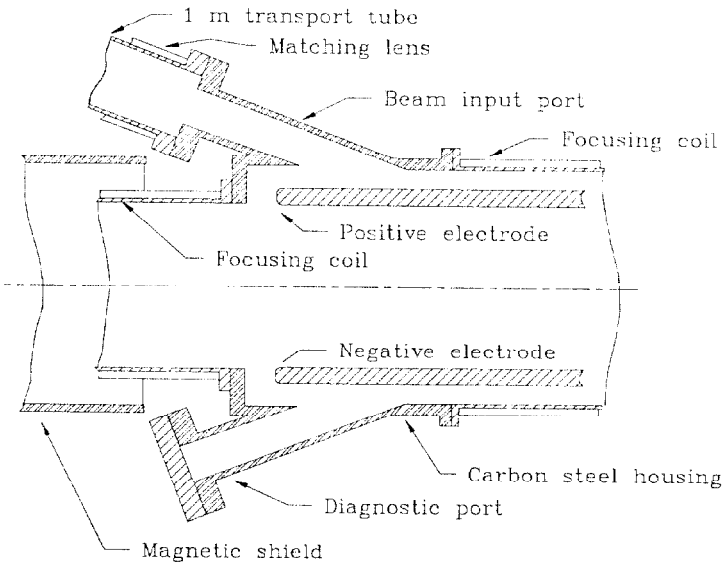

Fig. 3. Inflector assembly

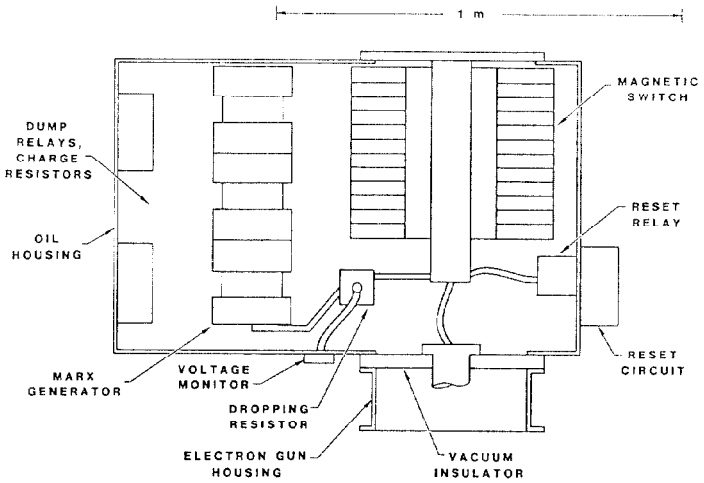

Fig. 4. Injector pulsed power system.

3. Injector experiments

The injector uses the novel pulsed power system illustrated in Fig. 4 to achieve a flat voltage waveform and high operational reliability. The electron gun is driven directly from a 300 kV Marx generator; the gun voltage is crowbarred after 80 ns by a saturable core magnetic switch consisting of 12 fast ferrite cores of 24 cm diameter. The combination of a reliable crowbar and good circuit damping allows reproducible beam generation with a simple felt surface cathode. The same cathode has been used for over 2000 shots at 1 kA/cm^2 with no degradation of current output. The injector can generate electron beams up to 1.5 kA with good voltage uniformity. Waveforms for the injector voltage and current available at the end of the 1 m transport tube are shown in Fig. 5. During the next year, the voltage of the injector will be raised to 600 kV by reconfiguring the magnetic switch as a 2:1 step-up transformer.

A series of beam propagation experiments were carried out using the injector and the 1 m transport tube. Results are reported in Ref. 6. A 290 A, 2.5 cm diameter beam was produced with a measured brightness of 2.6×10^8 $A/(m\text{-}rad)^2$. The beam was compressed for entry into the 1 m transport tube by a solenoidal lens. A well-directed beam of 150 A was transported through the tube. The polarity of the linear transport tube coils could be changed to generate both cusp fields and a straight solenoidal field. There was little observed difference in beam propagation characteristics for the two field geometries.

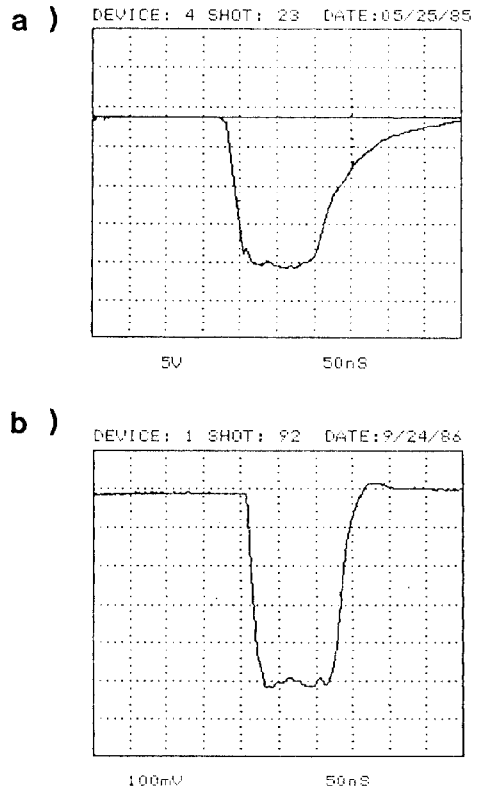

Fig. 5. Injector waveforms. a) Voltage, 70 kV/div, 50 ns/div. b) Current at exit of 3.2 m transport system, 22 A/div, 50 ns/div.

4. 180° sector experiments

A series of measurements on high current beam transport through a 180° sector of the main ring are reported in Ref. 7. The 300 kV beam from the injector was injected directly into the end of the sector. Detailed beam diagnostics could be performed in the open system. The main purpose of the experiments was to verify efficient transport in the 18 cell periodic focusing system and to make a direct comparison between cusp focusing and toroidal field focusing in a curved geometry. The polarity of adjacent focusing field coils was changed while maintaining constant parameters on the injector and matching optics.

As predicted, the periodic focusing system provided excellent containment of a 130 A beam at high vacuum. The rapidly reversing field polarity canceled transverse drift motions. In consequence, beam transport was quite tolerant to vertical field errors and system asymmetries. Fig. 6 indicates that a 100% vertical field error shifted 50% of the beam out of the acceptance of a 5.4 cm diameter current monitor at the downstream end of the transport tube. The optimum vertical field value corresponded to a match between the particle gyroradius and the 1 m radius of the transport system. Observations of the beam distribution at the end of the 3.2 m transport tube showed that field errors resulted in a horizontal shift of the beam centroid with little effect on the beam shape. The magnitude of the displacement was in agreement with theory.

In contrast, beam transport in a monodirectional toroidal field with 50% modulations was dominated by drift motions. Fig. 6 shows that collected beam current was reduced by 50% with only an 8% error. Beam distribution measurements showed that vertical field errors resulted in a distorted beam profile and large vertical displacements. The vertical field value corresponding to optimum beam transport was shifted up 50% compared to the value for cusp transport because of the effect of the grad-B drift. Beam displacements were in qualitative agreement with drift orbit theory. While the beam in the cusp array reached an approximate displacement equilibrium at the end of the transport tube, drift theory predicts that the beam in the toroidal field would suffer further displacement with increased system length. The actual tolerance on beam energy error in the modulated toroidal field is probably in the range 1-2%.

This work was supported by the Office of Naval Research under Contract No. N00014-84K-0248.

References

1. See, for instance, C.A. Kapetanakos, these proceedings.
2. S. Humphries, Jr. and D.M. Woodall, Bull. Am. Phys. Soc. 28, 1054 (1983).
3. H. Ishizuka, G. Leslie, B. Mandelbaum, A. Fisher, and N. Rostoker, IEEE Trans. Nucl. Sci. NS-32, 2727 (1985).
4. J. Golden, J. Pasour, D.E. Pershing, K. Smith, F. Mako, S. Slinker, F. Mora, N. Orick, R. Altes, A. Fliflet, P. Champney and C.A. Kapetanakos, IEEE Trans. Nucl. Sci. NS-30, 2114 (1983).
5. C.W. Roberson, A.A. Mondelli and D. Chernin, Phys. Rev. Lett. 50, 507 (1983).
6. S. Humphries, Jr., L.K. Len and C.B. Allen, to be published, Rev. Sci. Instrum.
7. S. Humphries, Jr. and L.K. Len, submitted to J. Appl. Phys.

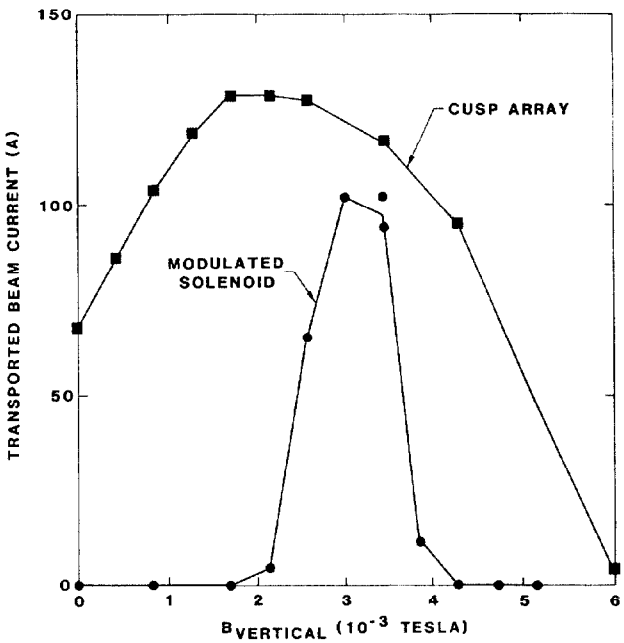

Fig. 6. Beam current detected at downstream end of 180° sector as a function of vertical field. Peak focusing field, 0.05 t.